We are IntechOpen,
the world's leading publisher of
Open Access books
Built by scientists, for scientists

6,900
Open access books available

185,000
International authors and editors

200M
Downloads

154
Countries delivered to

Our authors are among the

TOP 1%
most cited scientists

12.2%
Contributors from top 500 universities

CLARIVATE ANALYTICS
BOOK CITATION INDEX
INDEXED

WEB OF SCIENCE™

Selection of our books indexed in the Book Citation Index
in Web of Science™ Core Collection (BKCI)

Interested in publishing with us?
Contact book.department@intechopen.com

Numbers displayed above are based on latest data collected.
For more information visit www.intechopen.com

Observation and Research on the Typical Atmosphere of Beijing Olympic Games by Optical Remote Sensing

Wenqing Liu, Wei Huang, Pinhua Xie and Jianguo Liu
*State Environmental Protection Key Laboratory of Optical Monitoring Technology,
Ministry of Environmental Protection of the People's Republic of China,
Anhui Institute of Optics & Fine Mechanics, Chinese Academy of Sciences, Hefei, Anhui
P.R. China*

1. Introduction

The 29th Olympic and Paralympics Games were held from August 8th to September 17th, 2008 in China's capital – Beijing. Air quality is a critical concern to China and the world. To ensure good air quality during the Olympic Games, Beijing Municipal Government and the Environmental Protection Agency of China launched a program called "Air Quality Guarantee Plan for the 29th Olympics in Beijing (AQGP)". The period starting from July 1st, 2008 marked an intensified endeavour to improve Beijing's air quality by shutting down heavy polluters. 3.3 million motor vehicles were removed from city streets on alternate days, depending on whether the license plate ended in an odd or even number during the period of July 20th to Sep. 20th, 2008 (the alternative day-driving scheme). At the same time, the adjacent cities and provinces also did their best to close major polluters that may have influence on the air quality of Beijing. The exceptional strict pollution control measures have hugely reduced the source emissions, making a green Olympic Games achievable. Beijing's air quality has witnessed significant improvements due to enhanced pollution control efforts and new environment criteria.

Beijing's air quality was intensively monitored by environment protection authorities and research institutions before, during, and after the Olympic Games. The rich scientific data collected during the period have become solid evidences for judging the impact of exposure to air pollution on human health. To evaluate the effectiveness of the AQGP program, Beijing Municipal Environmental Protection Agency led a plan named "Assessment of AQGP and Air quality Monitoring, Forecasting and Early Warning".

There are numerous publications (Cermak & Knutti, 2009; Huang *et al.*, 2010; Y. Li *et al.*, 2010; X. G. Liu *et al.*, 2009; Mijling *et al.*, 2009; Shao *et al.*, 2009; Shen *et al.*, 2011; Shou-bin *et al.*, 2009; Simonich, 2009; Streets *et al.*, 2007; X. Y. Tang *et al.*, 2009; W. T. Wang *et al.*, 2009; Westerdahl *et al.*, 2009; Yao *et al.*, 2009) to now on evaluation of these pollution measures. Hou. et. al. (Hou *et al.*, 2010) measured the levels of Beijing residents' exposure to PM_{10} during three different time periods. Their study showed that during the Olympic Games, population-weighted PM_{10} exposure came down by 46% and 19%, respectively, compared with the pre-OG and the post-OG periods, indicating that in addition to favourable weather

conditions, enhanced traffic and emission control policies and measures have produced a noticeable effect on PM_{10} reduction.

For persistent organic pollutants (POPs), Zhang et. al. (L. F. Zhang *et al.*, 2010) systematic studied hexachlorobenzene in the ambient air before and after the Olympic Games. Hexachlorobenzene concentration was found decreased sharply in the winter of 2008 comparing with that of 2007 due to the implementation of a series of ''Green Olympic'' policies. Gas-particle partitioning shows that the increase of hexachlorobenzene levels in winter time was mainly contributed by the high total suspended particulate from combustion processes such as coal-burning and traffic emission.

Xin et. al. (Xin *et al.*, 2010) used Beijing-Tianjin-Hebei Atmospheric Environment Monitoring Network to monitor and provide warnings of the atmospheric quality in Beijing and its surrounding area during the Beijing 2008 Olympic Games. During the Olympic Games, the mean concentration of SO_2, $PM_{2.5}$, NO_2, O_3_8h max, and O_x were 12.5±4, 56±28, 23±4, 114±29, 95±17 μg/m³ in the region, respectively, and fell by 51.0%, 43.7%, 13%, 20.2%, and 18.9%, respectively, compared to the prophase mean concentration before the Olympic Games. After the Olympic Games, SO_2, $PM_{2.5}$ and NO_x increased significantly as the temporary atmospheric pollution control measures was terminated. Wang et. al's study (S. X. Wang *et al.*, 2010) showed that the mobile source NO_X and non-methane volatile organic compounds (NMVOC) reduced by 46% and 57%, respectively, during the Olympic Games period due to strict pollution policies.

Zhou et. al. investigated the effects of pollution measures on urban motor vehicle emissions in Beijing. (Zhou *et al.*, 2010) Comparison between the emission intensity before and during the 2008 Olympics shows a reduction of 44.5% and 49.0% in daily CO and NOx emission from motor vehicles. Their results suggest that reasonable traffic system improvement strategies along with vehicle technology improvements can contribute to controlling total motor vehicle emissions in Beijing after the Olympic Games. Wang et. al. (Wang & Xie, 2009) investigated the traffic-related air pollution in the urban streets. The average reduction of PM_{10}, CO, NO_2 and O_3 are 28%, 19.3%, 12.3%, and -25.2%, respectively. Another study (X. Wang *et al.*, 2009) evaluated on-road emission factors and black carbon profiles. Diesel trucks are believed to be a major source of summertime BC in Beijing. A mobile laboratory(M. Wang *et al.*, 2009) also was employed to evaluate changes in on-road air pollutants.

Liu et. al. (J. F. Liu *et al.*, 2009) measured the hourly concentrations of BTEX (Benzene, Toluene, Ethylbenzene, m,p-Xylene and o-Xylene) in the urban area of Beijing. They found that during the games, the mean daytime concentrations of benzene, toluene, ethylbenzene, m,p-xylene and o-xylene were 2.37, 3.97, 1.92, 3.51 and 1.90 μg/m³, respectively, and were 52.8%, 63.9%, 56.4%, 56.8%, and 46.9% lower than those after the games. Secondary pollutants and regional impact also were studied. (T. Wang *et al.*, 2010)

He et. al. (S. Z. He *et al.*, 2010) measured atmospheric H_2O_2 and organic peroxides in urban Beijing (at the Peking University campus), from 12th July to 30th September, before and during the Beijing Olympic Games full-scale control. They concluded that the heterogeneous removal of H_2O_2 is faster than that of methyl hydroperoxide (MHP), as indicated by the strong negative correlation between the H_2O_2–to–MHP ratio and the aerosol surface area.

Wang. et. al. (B. Wang *et al.*, 2010) assessed variation of ambient non-methane hydrocarbons by gas chromatography equipped with a quadrupole mass spectrometer and a flame ionization detector (GC/MSD/FID) as parts of the field Campaign for the Beijing Olympic Games Air Quality program (CareBeijing). Their findings demonstrate the effectiveness of

the air quality control measures enacted for the 2008 Olympics and indicate that controlling vehicular emissions could be the most important measure to improve the air quality of Beijing.

The abovementioned studies used all kinds of methods to evaluate the air quality during Beijing Olympic Games, but nearly none used optical remote sensing methods. Here we will introduce our investigations on the air quality of Beijing Olympic Games using all kinds of optical remote sensing techniques. Due to the limited room in this chapter, we will only introduce part of our results here.

The emission flux of important pollution sources was measured with mobile differential optical absorption spectroscopy (DOAS) and light detection and ranging (LIDAR). The sources are Capital Iron and Steel (CIS), Yanshan Petrochemical (YP), and Capital Airport (CA), respectively. It was found that CIS contributed most to emissions of NO_2, SO_2, and particulate matter, but the overall emission flux from June to September was decreasing, representing the effectiveness of air pollution control policy. It was also found that the emission flux came from YP declined as well, while the NO_2 emission of CA only had a slight drop.

The MAX-DOS system located in the region of pollution sources monitored the tropospheric column density of SO_2 and NO_2, which reflected the whole layer concentration of SO_2 and NO_2 around pollution sources. The results showed that the column density of SO_2 and NO_2 of CIS, YP and SO_2 decreased significantly, where the column density of NO_2 of CIS and YP decreased by 30-40%, whereas that of CA reduced less.

LIDAR measurements proved that emissions of particulate matter can be reduced to some extent by the alternative day-driving scheme and plant production restriction. Weather is the major factor for cleaning of particulate matters, implying that the emission control policy can only reduce the accumulation of pollutant in some extent, but the decisive factor of pollutant elimination is still weather.

The observation to 4 main pollutants (SO_2, NO_2, CO, PM_{10}) in all stations showed their concentration reached the China National Level II Standard and the guideline values of WHO. The concentration of NH_3 was found to be higher in the daytime while lower during the night-time. Varieties of optical remote sensing techniques were used to monitor the air quality of 2008 Beijing Olympic Games, and were proved to be critical in air quality monitoring system.

The tropospheric nitrogen dioxide over the Beijing Olympic Games venues was measured by ground-based Multi Axis Differential Optical Absorption Spectroscopy (MAX-DOAS), and was compared with the result of Ozone Monitoring Instrument (OMI) (Duncan *et al.*, 2010). It showed that the results of MAX-DOAS were higher than that of OMI, and can up to 2.4 times the result of OMI; both instruments had good correlation (r=0.64) when it is clear. There was more difference between the results of both instruments for the existing of cloud when it was rainy or cloudy, with a correlation coefficient of 0.19, but the results of MAX-DOAS had better consistency with LP-DOAS, with a correlation coefficient of 0.92.

2. Experimental methods - optical remote sensing

An integrated spatiotemporal monitoring system (Fig. 1) for regional complex air pollution was constructed which comprises a variety of optical remote sensing techniques, such as differential optical absorption spectroscopy (DOAS)(Winer & Biermann, 1994), light detection and ranging (LIDAR)(Vierling *et al.*, 2008), Fourier transform infrared

spectroscopy (FTIR)(Movasaghi *et al.*, 2008), tunable diode laser absorption spectroscopy (TDLAS) (Lackner, 2007), tapered element oscillating microbalance (TEOM) (Patashnick & Rupprecht, 1991). It was worth pointing out that all the instruments mentioned here were developed in our institute (Chen *et al.*, 2009; He *et al.*, 2009; Y. B. He *et al.*, 2010; Jin *et al.*, 2010; S. W. Li *et al.*, 2009; S. W. Li *et al.*, 2008; Lu *et al.*, 2010a, 2010b; Luo *et al.*, 2011; Si *et al.*, 2010; Y. Y. Tang *et al.*, 2010; J. Xu *et al.*, 2010; Z. Y. Xu *et al.*, 2010; S. A. Zhang *et al.*, 2009; Zhu *et al.*, 2010). We established 11 monitoring stations including 3 super monitoring stations and 2 mobile monitoring vehicles. From June 10th to September 20th of 2008, the air quality of Beijing area was monitored continuously and in real-time at these stations. Enormous data on all kinds of pollutants were acquired to assess the consequences of air pollution source control policies implied during the Olympic Games.

3. Experimental results and discussions

The integrated spatiotemporal monitoring system consists of 11 monitoring stations equipped with a variety of aforementioned optical remote sensing instruments. There are 3 super monitoring stations and 2 mobile monitoring vehicles. Air quality of Beijing area was monitored continuously and in real-time in these stations from June 10th to September 20th, Enormous data on all kinds of pollutants were acquired to assess the consequences of air pollution source control policies implied during the Olympic Games. Here we will choose some typical data to demonstrate applications of optical remote sensing techniques.
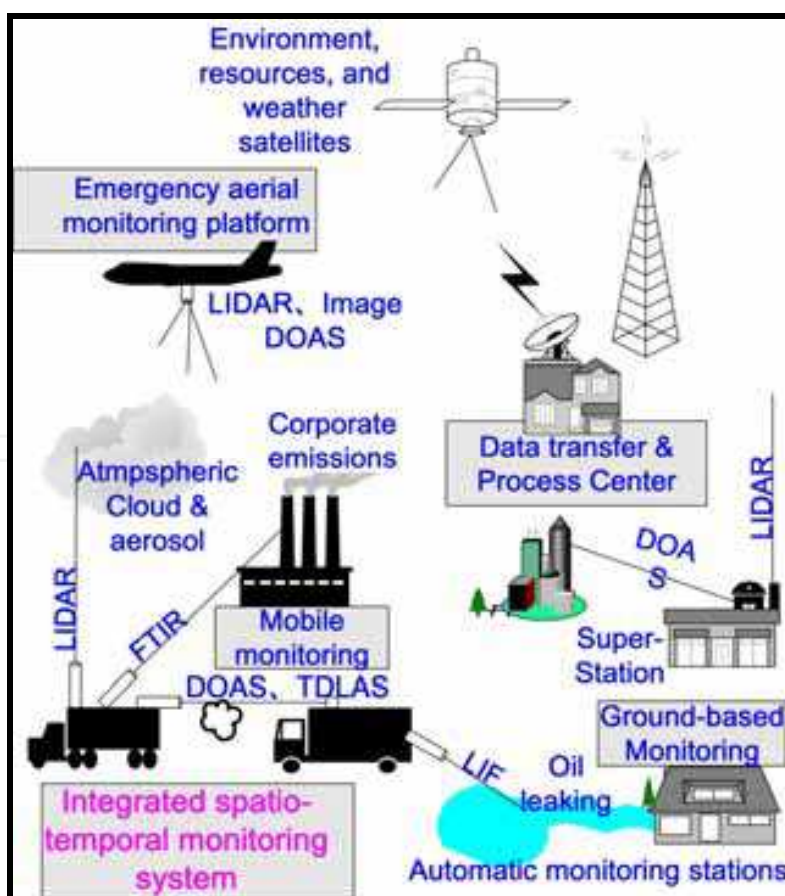

Fig. 1. Integrated spatiotemporal monitoring system for regional complex air pollution

3.1 Aerosol extinction & backscattering coefficients

We've done continuously measurements to air quality over the Olympic Games main sports center – "Bird's Nest" using double wavelength Raman LIDAR with three channels. The Raman LIDAR was installed at the Institute of Remote Sensing Applications (IRSA), Chinese Academy of Sciences, which is located about 500 meters north of the "Bird's Nest". The data acquired from Raman LIDAR are used to analyze the optical characteristics of representative weather during the period of Olympic Games.

Fig. 2 shows the aerosol extinction coefficient spatial and temporal distributions during Aug. 7th – Aug. 25th, 2010. Obviously, one can find that the aerosol extinction coefficients on Aug. 8th and Aug. 9th are considerably large, suggesting pretty heavy air pollution, and thereafter the atmosphere became clear due to several rainfalls.
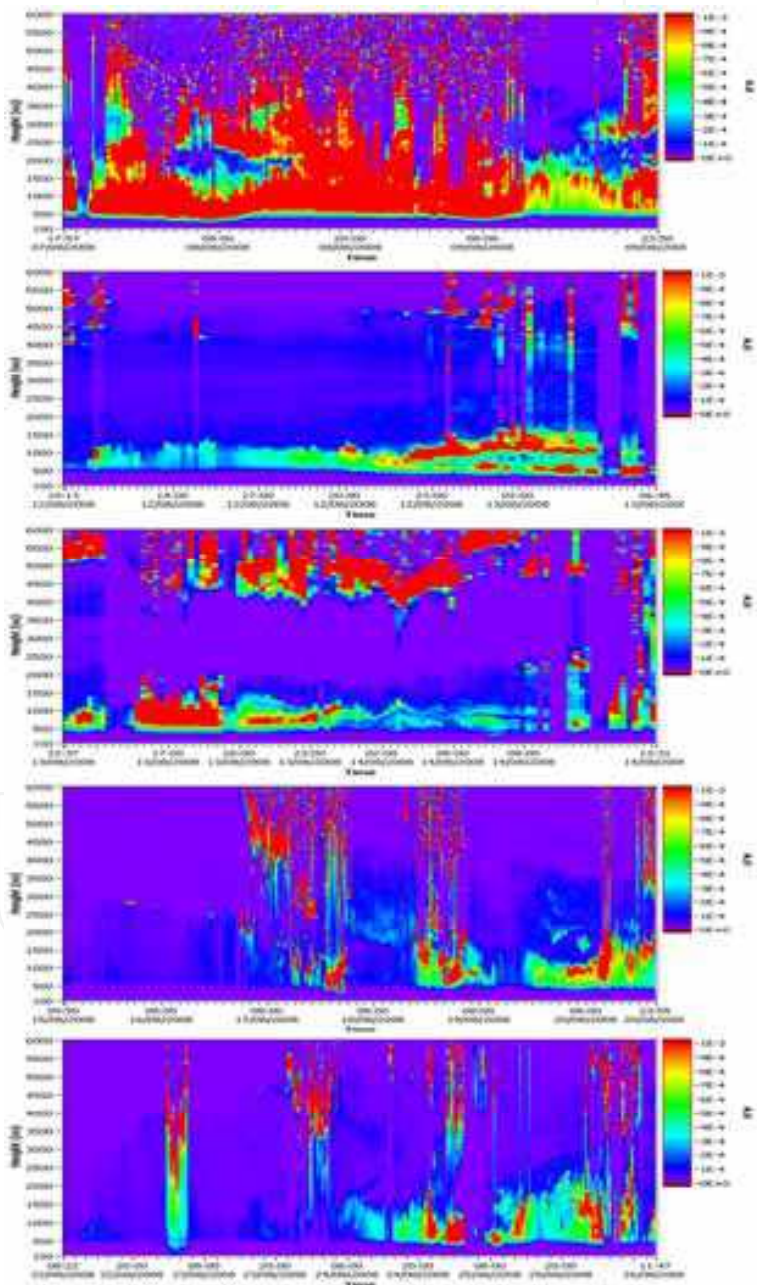
Fig. 2. Aerosol extinction coefficient vertical distributions during Aug. 7th ~ 25th, 2008

The aerosol extinction coefficient at some wavelength can give the distribution of pollutants, but it cannot provide the particle size information. Fig. 3 shows the spatial and temporal distribution of backscatter signal and extinction coefficient at 355 nm & 532 nm from Aug. 7th to 9th, 2010. As can be seen from the figure, the backscatter signals at 355 nm and 532 nm illustrate the spatial distribution of small aerosol particles clearly, and the heights of most of these small particles are lower than 600 meters. The most abundant distribution is at ~400 meters, and this is verified by the ratio of aerosol extinction coefficients at two different wavelengths. The height distribution and diurnal change of boundary layer are clearly demonstrated in the spatial -temporal distribution (Fig. 3).
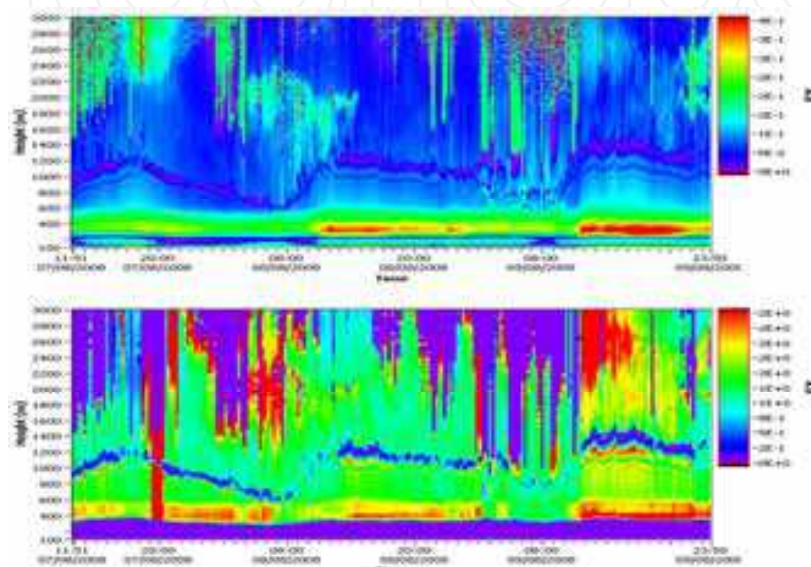
Fig. 3. Ratio vertical distribution of backscatter signal (upper pannel) and extinction coefficient (lower pannel) of 355/532 nm from Aug. 7th to 9th, 2008

It is worth noting that Yang (Yang *et al.*, 2010) also used a Dual-wavelength Polarized LIDAR to analyzes the variation of aerosol extinction coefficients during the Beijing Olympic Games. Their results showed that (1) during the Beijing Olympic Games, the aerosol extinction coefficient decreased to about 42.3% in the surface layer (below 250 m) compared with that in 2007 under almost the same meteorological conditions, indicating the effectiveness of local air pollution control measures in Beijing areas; (2) the analysis of the aerosol extinction coefficient obtained before (Jul. 20th–Aug. 7th, 2008) and during the Beijing Olympic Games (Aug. 8th–Aug. 24th, 2008) shows a maximum decrease of daily aerosol extinction coefficient in the layer of 0.5−1.5 km. To elucidate such a phenomenon, the transport of PM_{10} from surrounding areas to Beijing was simulated by NAQPMS (the Nested Air Quality Prediction Modeling System) for the period from Jul. 20th to Aug. 24th, 2008. Analysis of PM_{10} transport from neighboring areas indicated a decrease of 36.6% during the Olympic Games.

Aerosol optical depth (AOD) is a manifestation of air pollution to some extent, and angstrom wavelength exponent (AE) is an indicator of the relative size of aerosol particles. Fig. 4 illustrates the distribution of aerosol optical depth and angstrom exponent between Aug. 7th and Aug. 25th, 2010. One can clearly see that the AODs in the first 3 days are large, and the AOD of Aug. 8th is much larger. The data of Aug. 10th, Aug. 11th, Aug 14th, and Aug. 21st are missed due to rains in these days. According to the variations of AOD, we found

that the AOD rose significantly after rainfalls, hinting a procedure of pollutants accumulation. The average Angstrom exponents calculated from Fig. 4 is 2.64. Fig. 4 shows that the heavy pollution on Aug 8th-9th is caused by large aerosol particles. The AEs are very small after the rainfalls on Aug 14th and Aug. 21st, meaning the average aerosol particle size is small, and this agrees well with other atmospheric fine particle size measurements.
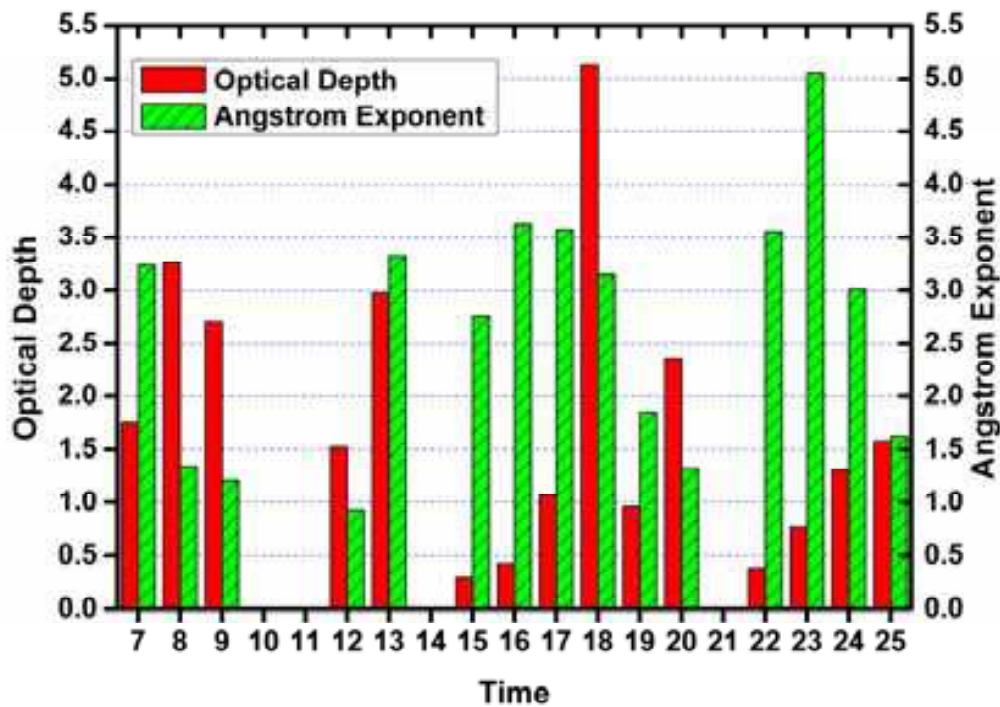

Fig. 4. Distribution of aerosol optical depth and Angstrom exponent during 20:00~23:59 during Aug. 7th ~ 25th, 2008

From the measurements of Raman LIDAR, it was concluded that: (a) the distribution of pollutants on Aug 7-9th exhibits period variation with time, and the heavy pollution on Aug. 8-9th is attributed to large aerosol particles; (b) The echo signals of LIDAR at different wavelengths clearly depicts the spatial distribution of aerosol particle size. The altitude of most small particles is about 400 meters. The AOD become much larger after rains, suggesting an accumulation process of pollutants; (c) the average AE is 2.64 during the period of Olympic Games, and its diurnal changes are in very good agreement with the data of ground-based atmospheric fine particle measurement.

3.2 Measurement of SO$_2$, NO$_2$, O$_3$ and PM$_{10}$

5 of the 11 monitor stations are used to measure the conventional pollutants in Beijing and surrounding areas. These stations are located in Yanshan Petrochemical (YP), Yugang Town (YT), Institute of Remote Sensing Applications, Chinese Academy of Sciences (IRSA), Capital Airport (CA), and Yongledian Town (YLD), respectively. The concentration of gaseous pollutants, i.e., SO$_2$, NO$_2$, and O$_3$, was measured using DOAS. We tested the performance of the DOAS system and calibrateed the lamp spectra every day. The comparison of these data with other instruments in IRSA and YP was used to ensure the accuracy and reliability of field measurements. TEOM was used to get the PM$_{10}$ data. The

measurements started from Jun. 20th of 2008, and ended in September, 2008. We will introduce the time series, average diurnal change, regional transport, and comparison of pollutant concentration in YP, YT, IRSA, and CA.

3.2.1 Time series of pollutant concentration

Fig. 5 is the hourly average time series of pollutants. The PM_{10} concentration of IRSA station is much higher than that of YT because IRSA is very close to the Bird's Nest, and there were more human activities near this station, while YT is in suburb area. The maximum concentration of PM_{10} in IRSA station occurred at 13:00, July 4th, and is 470.6 µg/m³. The maximum concentration of PM_{10} in YT station occurred at 22:00, July 27th, and is 354.0 µg/m³. The sources of PM_{10} are very complicated, e.g., coal and dust pollution, industrial emissions, vehicle emissions, and pollutants transport. The weak southerly wind from July 4th to Aug. 10th hindered the diffusion of pollutants, and made the concentrations of PM_{10} and O_3 measured in each station are pretty high.

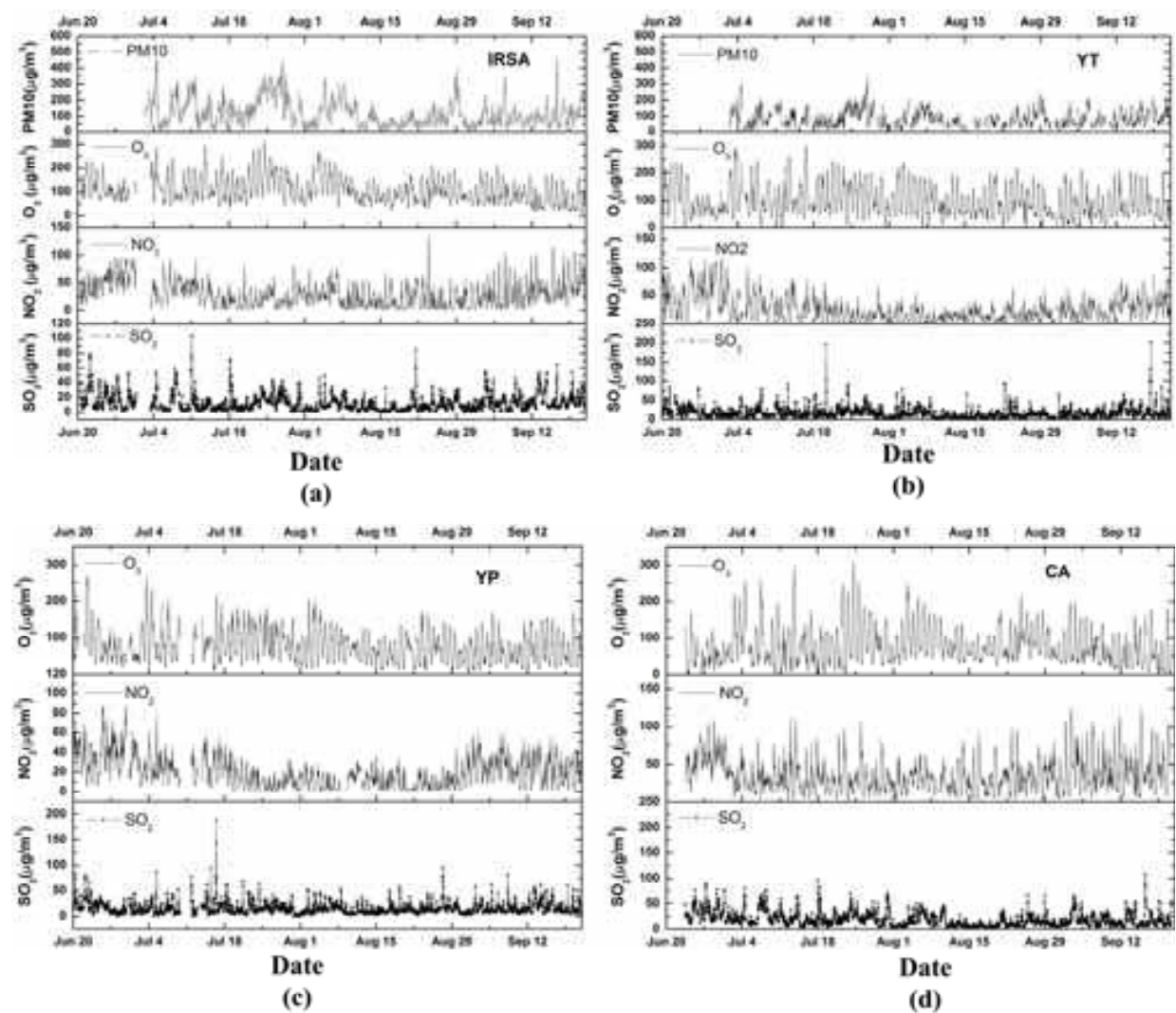Fig. 5. Time series of observed SO2, NO2, O3 and PM10

O_3 came from the photochemical reactions during the daytime, and exhibited apparent diurnal variation trend, i.e., the peak value occurred in the afternoon, as the valley

happened in the night. The maximum hourly average O_3 concentration occurred at 13:00, Jun. 22nd in IRSA station, and the value is 324 µg/m³. The concentrations of SO_2 and NO_2 were under the requirement of National Atmosphere Environment Quality Level II, which are 500 µg/m³ and 120 µg/m³. The main source of SO_2 came from combustion of sulfur compounds. The peak values of SO_2 concentration were more frequently found in YP and YT stations. NO_2 was found to have a contrary trend with O_3 in concentration change, i.e., the concentration was high during the night, but became lower in the day due to low photolysis concentration. There are lots of rainy days before July due to Mongolian cold- and low-swirl. In addition, the emission reduction policy started to effect since July. These two factors caused the concentration of NO_2 generally was high as a result of lacking of photolysis. The concentrations of primary pollutants, SO_2 and NO_2, have significant falling with the implementation of emission reduction policy, particularly during the Olympic Games period.

3.2.2 Diurnal variation of pollutants in different monitoring sites

Fig. 6 presents the average diurnal variations of SO_2, NO_2, O_3, and PM_{10} at different monitoring sites in different stages. The average diurnal variation curves of urban site (Fig. 6a, IRSA) and suburban site (Fig. 6b, YT) show that the concentration of PM_{10} only changed slightly, and the PM_{10} concentration of IRSA site is higher than that of YT site. The PM_{10} concentration measured in IRSA site was found decreasing continuously from Jul. 20th (The alternative day-driving scheme starting date) to September. The sharpest decreasing occurred between 01:00 ~ 12:00, and the PM_{10} concentration average diurnal variations at other stages were nearly equal. The PM_{10} concentration measured at YT site had a significant decline in September than before, and the main difference happened between 02:00 ~ 10:00. The average difference between urban and suburban changed from 50% of Jul. 1st – Jul. 19th to 25% of Sept. 6th – Sept. 17th.

The measured NO_2 concentration in all the monitor sites exhibited lower value from Jul. 20th to Aug. 24th. The diurnal variation has an obvious double-peak. The first peak appeared at 05:00 ~ 09:00, suggesting that it may be related with local traffic emission and human activity. The second peak came out at 19:00 ~ 22:00, and this is originated from concentration accumulation due to atmospheric inversion effects of near-ground atmosphere and lack of photolysis in the night.

The comparison of NO_2 diurnal variations in different monitoring sites showed that the concentration of NO_2 in Capital Airport (CA) changed very little. This is reasonable when considering the large number of air flights every day, and the effect of alternative day-driving scheme is relative small. The measured NO_2 concentration in July is much lower than that of June, and there is no clear peak value in the morning. The NO_2 concentration of all sites during Sept. 6th –Sept. 16th increased a little bit compare with previous measurements, especially at around 19:00 in Capital Airport and 21:00 in IRSA.

The NO_2 concentrations were found to decrease most in IRSA and CA sits from the average diurnal variation of SO_2. The intermittent SO_2 peaks appeared in YT site (16:00) before applying alternative day-driving scheme and YP site (10:00) during Jul. 1st – Jul. 19th. The NO_2 average diurnal variations generally showed single peak, and only YP and YT sites showed double-peak. The NO_2 concentration is higher during the night-time in urban sites, while high NO_2 concentration was found in other sites, e.g., YT and YP sites were found to have peak value between 07:00 ~ 09:00.
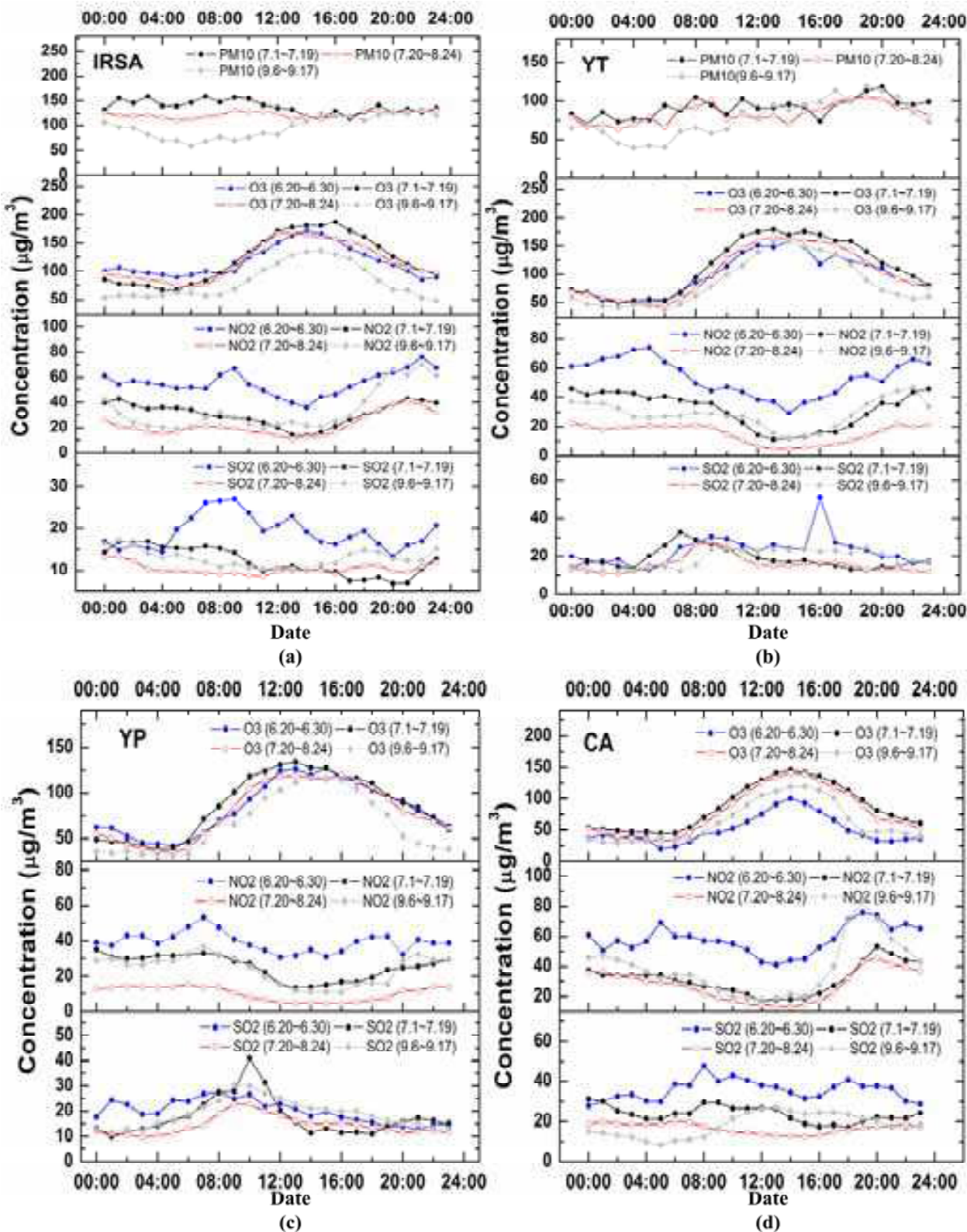
Fig. 6. Average diurnal patterns of SO_2, NO_2, O_3 and PM_{10} in 4 monitoring stations

In contrast with NO_2 and SO_2, the measured O_3 concentration increased somewhat at the beginning of applying alternative day-driving scheme. This can be explained by that O_3's originate in Beijing is basically controlled by VOCs. The decreasing of NOx resulted in local

Observation and Research on the Typical Atmosphere
of Beijing Olympic Games by Optical Remote Sensing
165

O_3's consumption declination too, thus caused the increasing of O_3 concentration. The statistic data after Jul. 20th demonstrated that the O_3 concentration decreased continuously. O_3 concentration exhibits typical diurnal variation pattern, that is, the peak value appeared in the daytime, while the concentration became lower due to the reaction with NO. Measurements in urban sites showed that the O_3 concentrations in Jul. 20th - Aug. 24th are comparable to that of June, but slightly lower. The peak O_3 concentration appeared earlier from 16:00 of Jul. 1st - Jul. 19th to 13:00 of Jul. 20th - Aug. 24th, while the peak appeared time from Sept. 6th – Sept. 17th is almost the same as that the beginning of alternative day-driving scheme and the difference between peak and valley values became smaller and smaller. O_3 concentrations measured in YP and YT sites gave apparent double-peak features, where the first peak appeared around 13:00, and the second peak appeared around 16:00. The second peak probably is related with O_3's regional transport. Although YT site is far from urban area, O_3 concentration was found to increase at the beginning stage of alternative day-driving scheme, but it became much lower afterwards, and the second peak became not so obvious. We found the same trend for O_3 in Capital Airport, whose peak value appeared at around 14:00. The maximum concentration of O_3 during Jul. 1st - Jul. 19th increased by nearly 40 µg/m³ compare with that of June, and become a little lower afterwards.

3.2.3 Observation of pollutants regional transport

We will take the measured data of Aug. 8th in four sites as an example to investigate the effect of the regional transport in southwest direction. SO_2 and O_3 were chosen as tracer pollutants. Fig. 7 shows the air mass backward trajectory at 200 m, 500 m, and 1000 m heights in 24 hours using HYSPLIT model, where the star labeled the location of IRSA. One can find from Fig. 7 that the main wind direction is southwest, and the air mass transportation is from southwest (YP) to northeast (IRSA).
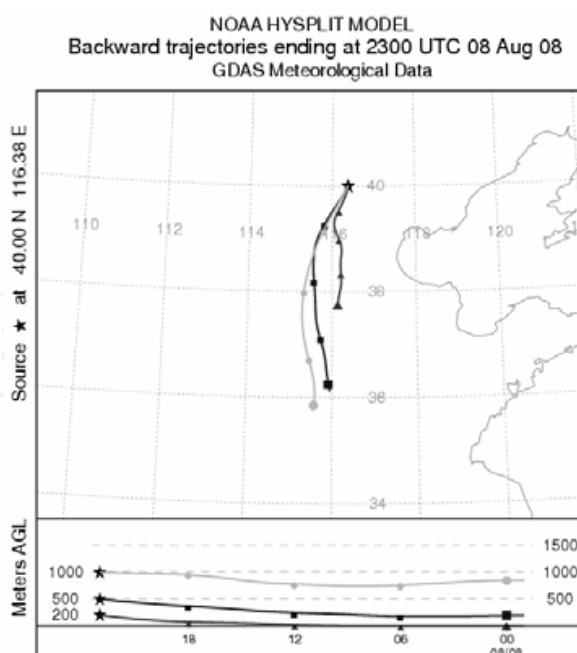

Fig. 7. Air trajectories for different altitudes of Aug. 8th, 2008

Fig. 8 presents the diurnal variations of SO_2 and O_3 on Aug. 8th, 2008. The YP monitor site got SO_2 peak value at 12:00 first, and then the peak values were found in YT, IRSA, and CA

sites at 13:00, 14:00, and 15:00, respectively. The time gap between the peak values is about 1 hour. SO_2 was found to move from southwest (YP) to northwest (IRSA, CA). Same as SO_2, the O_3 peak value was found in YP site (12:00), and then YT, IRSA, and CA sites. The delay between peaks is about 1 hour as well. The O_3 concentration of YP site was found to be the lowest, and keep at 125-128 µg/m³ level during 12:00-16:00, and lowered a little bit at night-time, but the second clear peak was found after 21:00. YT and IRSA sites then found O_3 concentration peak values during night-time at 22:00 and 23:00, respectively. These peak values may be related with pollutants regional transport. Such findings are consistent with the SO_2 vertical column density measurements of MAX-DOAS.
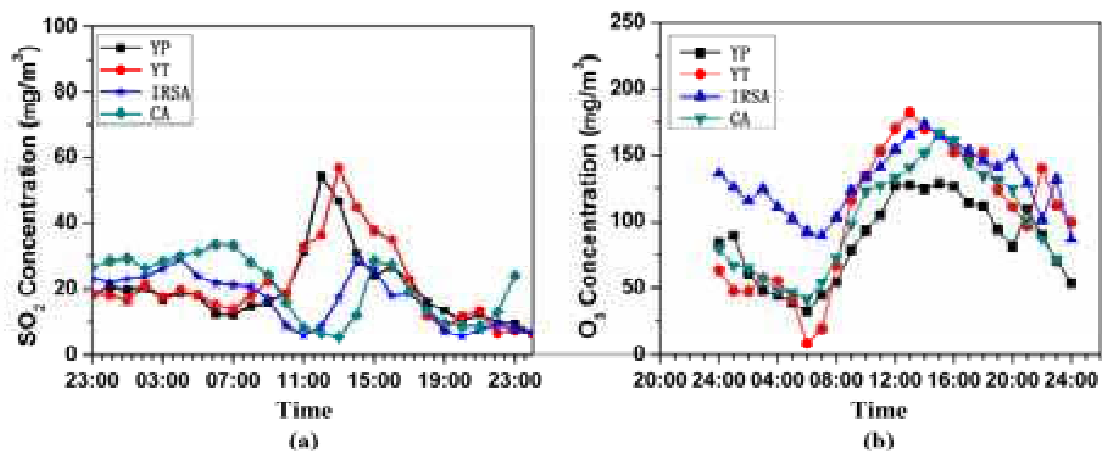

Fig. 8. Diurnal variation of SO_2 (a) and O_3 (b) measured at 4 monitoring stations on Aug. 8th, 2008

3.2.4 Comparison of pollutants concentration in different monitoring sites

Here we present the diurnal averages of PM_{10}, SO_2, and NO_2 concentration; the maximum hourly average concentration of O_3 measured during Jun. 20th – Sept. 22nd in every monitoring site. Table 1 gives the concentrations of conventional pollutants, PM_{10}, SO_2, NO_2 and O_3, measured at different stages between June and September, 2008, where diurnal averages value were used for PM_{10}, SO_2, and NO_2, while maximum hourly average values were used for O_3.

PM10: Fig. 9 presents the comparison of PM_{10} daily average concentration and statistical diurnal average concentration measured in IRSA and YT sites. Since IRSA site is close to the Bird's Nest and there are more human activities around the site, the concentration measured here was about 40% higher than that of YT site. The PM_{10} variation patterns in two sites are similar, and high concentration was found in two periods (Jul. 24th – Jul. 28th, Aug. 4th –Aug. 7th). The respirable particulate matters accumulate due to the static stable weather and resulted in the PM_{10} concentration in IRSA exceeded the National Atmospheric Environmental Level II standard (150 µg/m³). We can see from Table 1 that the PM_{10} concentration of IRSA which located in urban area was larger than that of YT, and the reductions were 12.1% and 9.9%, respectively. The measurements at urban sites showed that of PM_{10} concentration had a big growth in September.

SO_2: Fig. 10 presents the variation of NO_2 daily average concentration and the contrast of statistical average concentration. No concentration over standard was found during the whole campaign. Since there were lots of precipitations between Jun. 28th and Jul. 4th, the concentrations of pollutants like NO_2 were relatively low due to wet sedimentation. The NO_2 concentration of CA was higher than other sites, and the highest concentration
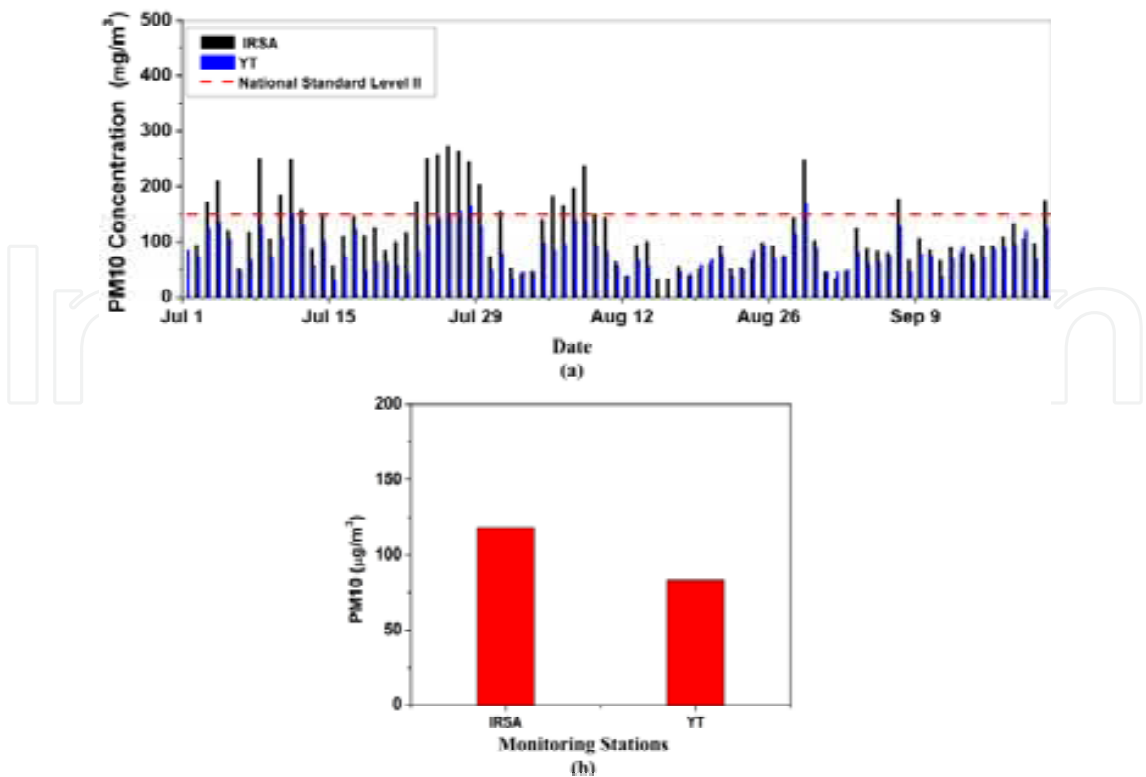
Fig. 9. Diurnal mean variation (a) and statistical average daily mean of PM_{10} concentration (b) during the campaign

Site	Pollutants ($\mu g/m^3$)	Measurement Periods							
		June	7.1-7.19	7.20-8.24	8.8-8.24	9.6-9.17	7.1-7.19/June Decease	7.20-8.24/7.1-7.19 Decrease	9.6-9.17/8.8-8.24 Decrease
YT	NO_2	51.7	32.0	15.6	13.9	28.6	38.1%	51.3%	-105.6%
	SO_2	22.7	18.2	15.6	11.4	18.5	19.8%	14.3%	-61.7%
	O_3	176.1	200.4	177.8	155.9	166.1	-13.8%	11.3%	-4.03%
	PM10		90.0	81.3	66.3	75.9		9.6%	-14.5%
IRSA	NO_2	54.5	33.2	21.9	18.7	32.8	39.1%	34.0%	-75.8%
	SO_2	19.4	12.3	10.2	7.7	15.1	36.6%	17.1%	-97.0%
	O_3	185.0	208.3	179.7	136.8	144.7	-12.6%	13.7%	-2.5%
	PM10		139.0	122.2	80.8	94.4		12.1%	-16.9%
YP	NO_2	37.8	26.6	10.3	10.1	24.1	29.6%	61.3%	-142.5%
	SO_2	19.1	18.4	14.4	12.6	18.8	3.7%	21.7%	-50.0%
	O_3	145.4	157.4	135.7	111.6	125.0	-8.3%	13.8%	-8.9%
CA	NO_2	57.8	32.5	27.5	28.4	20.5	43.8%	15.4%	-35.8%
	SO_2	37.2	25.1	16.8	10.7	18.1	32.5%	33.1%	-68.3%
	O_3	106.0	157.6	153.7	124.1	129.7	-48.7%	2.5%	-3.3%

Table 1. Concentrations of routine pollutants at 4 monitoring stations from June to September, 2008

measured on Jun. 27th was 56.8 µg/m³. The average concentrations of each site was found to decrease more than that before implementation of alternative day-driving scheme, especially for IRSA site where the reduction up to 35%. Due to the continuous rain showers between Aug. 8th and Aug. 15th, the NO_2 concentrations in several sites were found decreased considerably because of NO_2 purge. CA's SO_2 concentration decreased significantly during the period of Jul. 20th – Aug. 24th compare with the beginning of the alternative day-driving scheme. After the Olympic Games, the SO_2 concentrations measured in all sites were higher than that of August. Specifically, the concentration of SO_2 was found to increase by 97% (Table 2). One can find the CA statistical diurnal average concentration is the highest in all the sites, followed by YT, YP and IRSA. This can be explained by there are more flights in CA area.
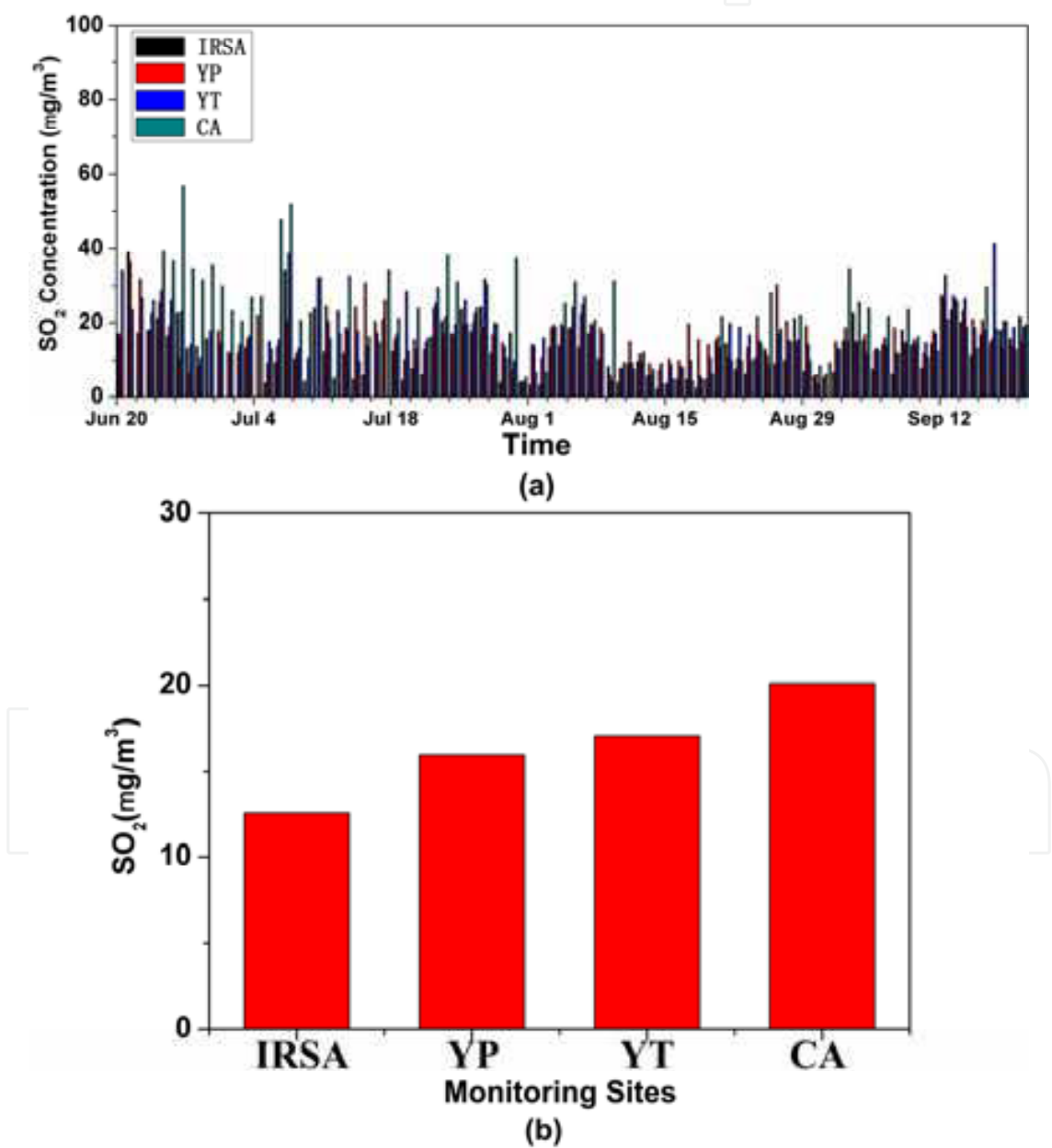

Fig. 10. Daily mean variation and statistical average daily mean of SO_2 during the whole campaign

NO₂: Fig. 11 gives the NO_2 diurnal average concentration and the comparison of statistical average concentration. Same as SO_2, there was no concentration over standard was found. There were lots of rains between Jun. 25th and Jul. 1st. NO_2 accumulated due to lack of photolysis in this period, and resulted in high concentration during Jun. 27th and Jun. 29th. As the weather changed and photochemical activity was enhanced after Jul. 1st, the NO_2 was decomposed through photolysis and NO_2 concentrations at all sites decreased. The static weather pollutants accumulated on Jul. 29th and Aug. 1st-Aug. 8th resulted in high NO_2 concentration. With the coming of Olympic Games opening ceremony, the NO_2 concentration in CA and IRSA increased gradually, but decreased abruptly on Aug. 8th. Same as that of SO_2, NO_2 concentration in BA site was higher than other sites. With the implementation of emission reduction policy, NO_2 concentration in YP and YT decreased noticeably during Jul. 20th to Aug. 24th. The concentration in all sites increased to some extent in September, especially in YP and YT sites, and the growths are 142% and 105%, respectively. Judged from statistical diurnal average concentration, CA and IRSA had a higher NO_2 concentration due to human activity, then followed by YT and YP.
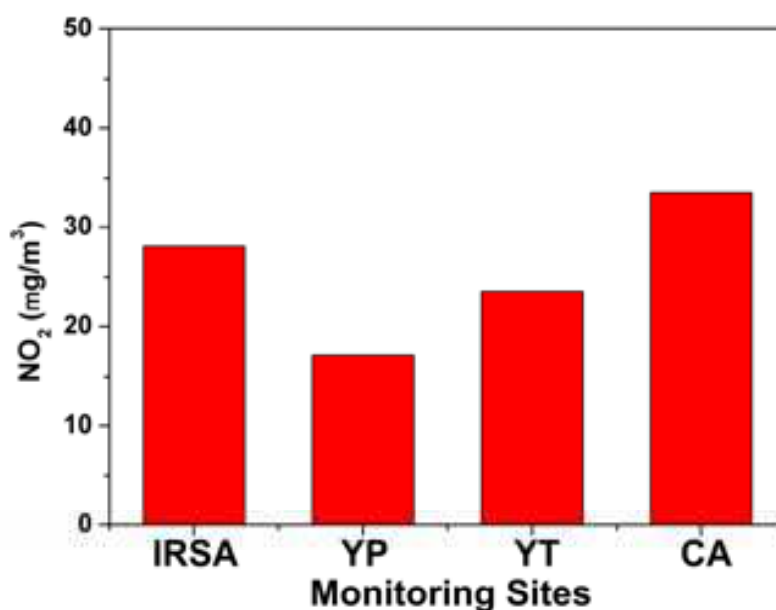

Fig. 11. Daily mean variation and statistical average daily mean of NO_2 during the whole campaign

O₃: Fig. 12 gives the O_3 diurnal hourly concentration and the comparison of statistical hourly maximum average concentration. As a result of rainy weather, the low photochemical activities led to low O_3 concentration. The concentration exceeding standard happened mainly during the static stable weather period, and they are Jul. 11th – Jul. 25th, and Aug. 2nd – Aug. 6th. In particular, the O_3 concentration in several sites increased at a rate of about 40% from Aug. 1st to Aug. 6th with the maximum happened on Aug. 3rd, and then decreased at a rate of 7%/day. From Aug. 8th to the end of Olympic Games, O_3 concentration measured in 4 sites meet the National Air Quality Standard Level II overall and were kept in a relative low level except on some days. From the statistical hourly average maximum concentration, YT site had the highest O_3 concentration, followed by IRSA and CA, and YP had the lowest O_3 concentration.
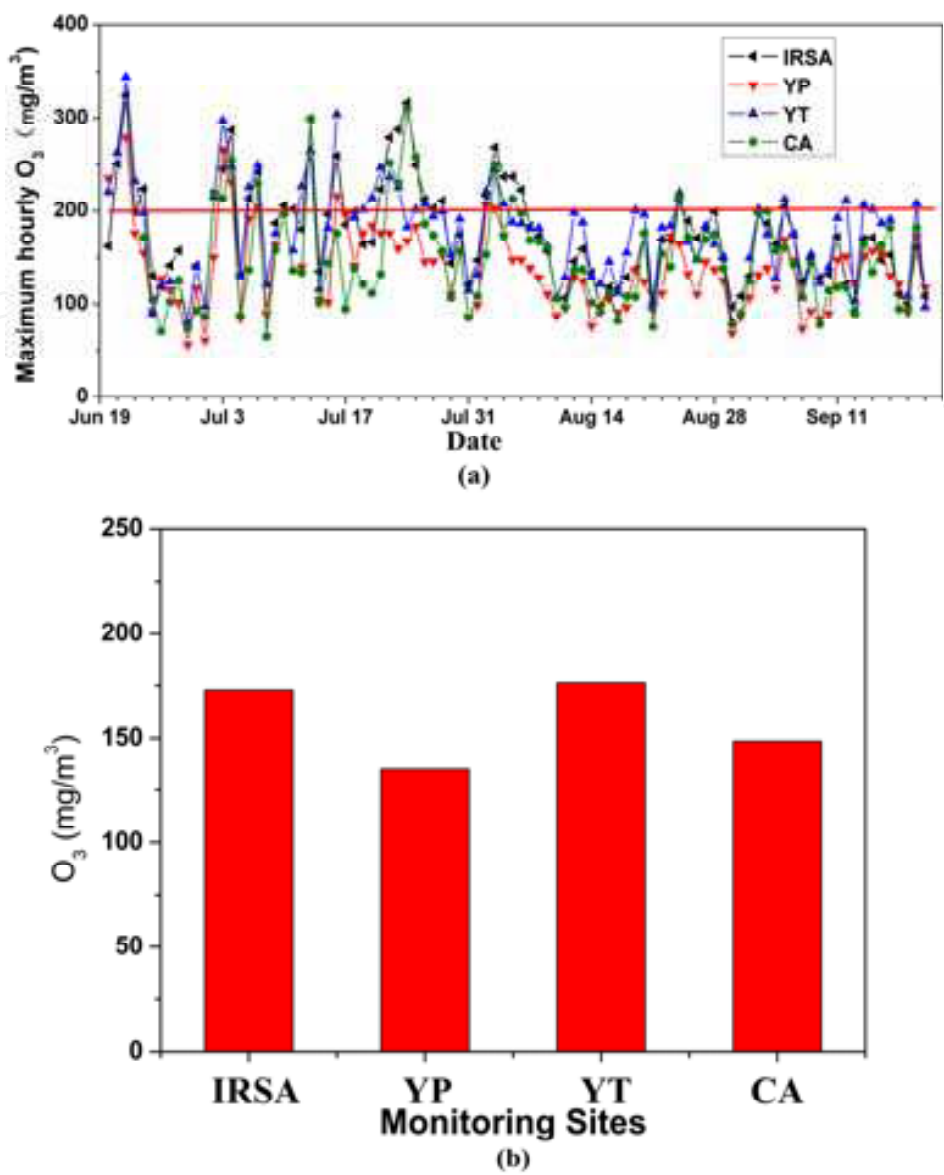
Fig. 12. Maximum hourly ozone concentrations on a daily basis and statistical average of the maximum hourly ozone during the whole campaign

The exceeding standard hourage of each site is shown in Fig. 20. One can find that O_3 concentrations go beyond the standard on Jun. 22nd, Jul. 3rd - Jul. 4th, Jul. 7th, and Jul. 16th. It is worth to mention that the period over standard in YP, YT and IRSA on Jun. 22nd was found to last up to 9 hours. With the implementation of pollution reduction policy, O_3 concentration in YP decreased significantly. The O_3 concentration in all sites meet the requirement of National Air Quality Standard Level II except O_3 concentration of YT site exceeded the standard occasionally.

SO_2 and NO_2 concentrations were found to meet the National Air Quality Level II standard during the whole campaign. The SO_2 and NO_2 concentration declined in the first stage of alternative day-driving scheme (Jul. 1st – Jul. 19th). The reduction of NO_2 was far larger than that of SO_2, and reduced up to 30% in all the sites, especially in CA site. All the pollutants concentration continue to decrease in the second stage (Jul. 20th – Aug. 24th), and NO_2 concentration in YP site which is in suburban decreased most significantly and up to 60%,

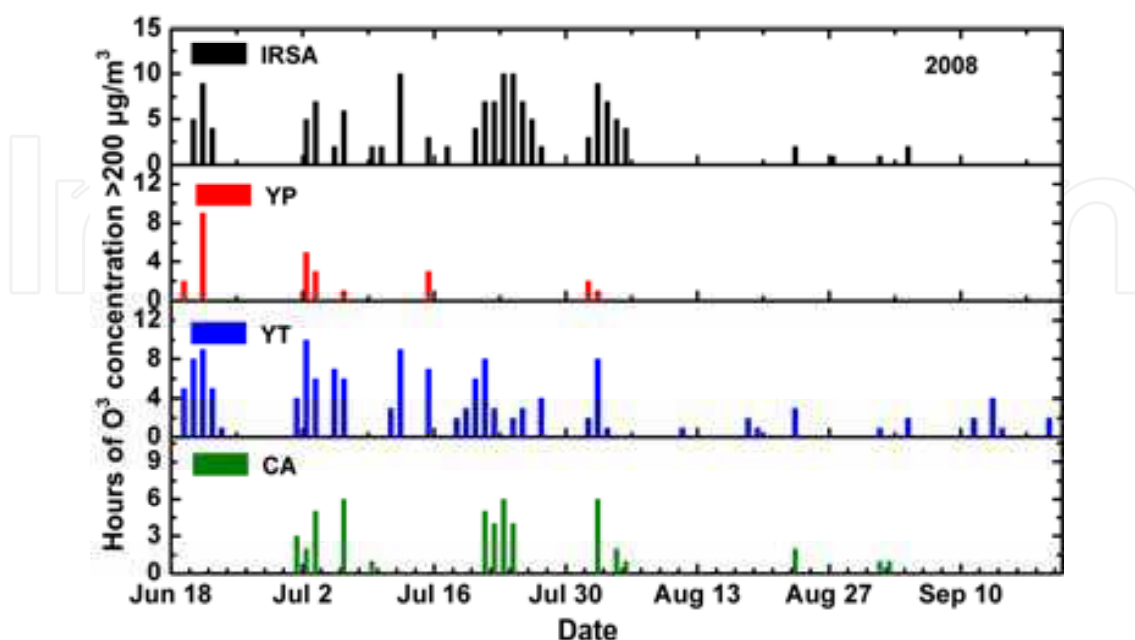then followed by YT site. The SO_2 concentration in CA site decreased most drastically and up to 33%.

Fig. 13. Hourage of O_3 exceeding standard

The O_3 concentration was found to go up then go down at the beginning of the alternative day-driving scheme. This can be explained by that Beijing is located in the VOCs control area generated by O_3. The reduction of NOx due to alternative day-driving scheme will cause O_3 concentration to increase. Compare with June, O_3 in CA site increase most significant and up to 48.7%, and that of YT and IRSA increase by about 13%. The regional transport existed due to the influence of the southwest wind. The YT and IRSA sites located in the downwind of YP site can find peak O_3 in turn.

Since PM_{10} is more closely affected by human activities, the PM_{10} concentrations in monitoring sites in urban area were higher. The PM_{10} concentrations of IRSA which is in urban area were found to have more reduction than that of YT site during the Olympic Games period compare to the first stage, and decreased by 12.1% and 9.6%, respectively.

When comparing the Olympic Games period with the first stage of emission reduction policy, SO_2, NO_2, O_3, and PM_{10} concentrations in all monitoring sites decreased by 14%-33%, 15%-6%, 2.5%-14%, 10%-12%, respectively. But the concentrations of these pollutants increased during the Paralympic Games period.

3.3 Comparison of NO₂ measured by MAX-DOAS and OMI

Fig. 14 presents the comparison of the tropospheric NO_2 colmun density of MAX-DOAS and OMI from Jun. 10th to Sept. 14th. The MAX-DOAS setup was installed close to the Bird's Nest. One can easily find the results of ground-basd MAX-DOAS are higher than that of OMI, and can up to 2.4 times on some days (Fig. 14a). This can be explained by spatial resolution difference between MAX-DOAS and OMI. The OMI's spatial resolution is 13×24 km² whereas MAX-DOAS has much higher resolution. This means the results of OMI is the average of a large area including the urban and suburban area. We know that the NO_2 of suburban area is much lower than that of urban area. This was validated by the average

NO$_2$ column density measured in 3 sites (Fig. 14b). Fig. 14b showed the column density ratio of MAX-DOAS to OMI decrease to 1.5 - 1.8 (Table 2). One can image that with more sites, the MAX-DOAS average will be close to OMI measurements.

	OMI (10^{15}molec./cm^2)	MAX-DOAS (10^{15}molec./cm^2)	Average (10^{15}molec./cm^2)
June	8.54	12.46	13.13
August	7.81	15.91	14.36
September	9.05	19.91	15.36

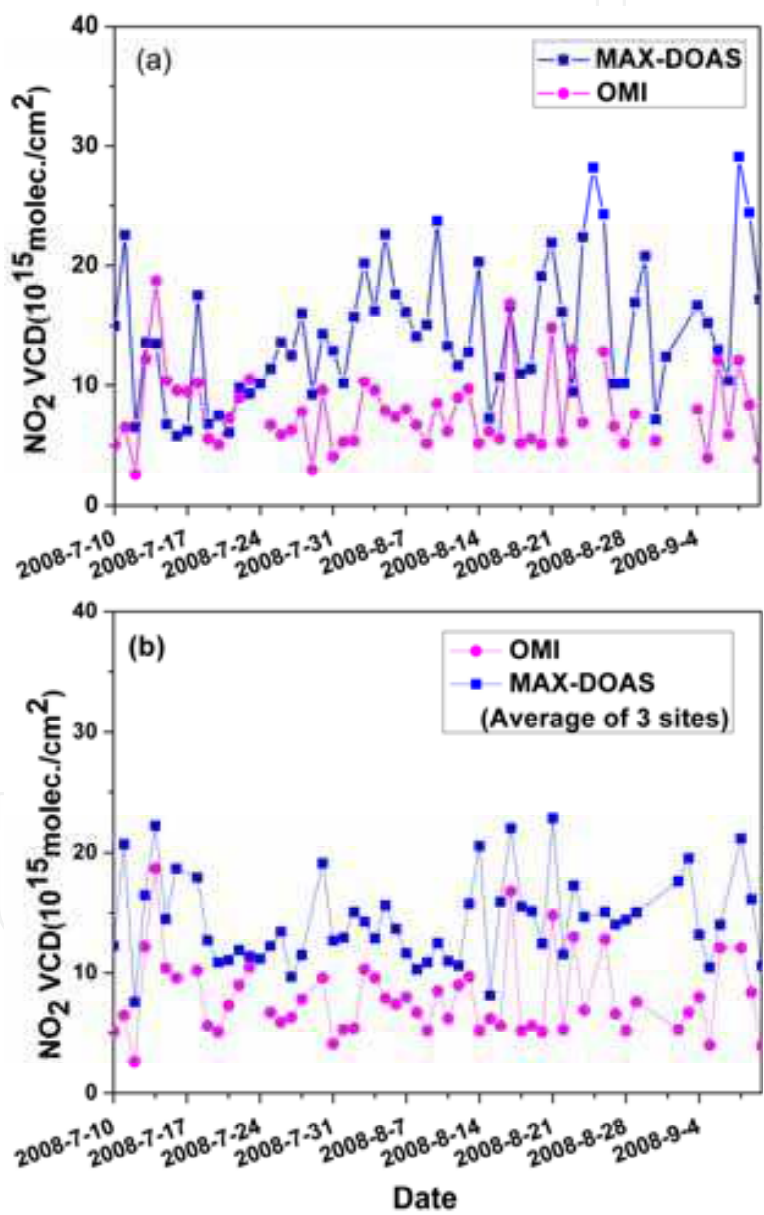Table 2. Comparison of monthly average between OMI and MAX-DOAS

Fig. 14. Comparison between the results of OMI and MAX-DOAS,(a) is the result of comparison between OMI and MAX-DOAS near the Olympic venues,(b) is comparison between OMI and the average of three sites, IRSA, CIS and YT, which are in the same pixel of OMI

Observation and Research on the Typical Atmosphere
of Beijing Olympic Games by Optical Remote Sensing
173

It is worth to mention that Yu (Yu *et al.*, 2010) also assessed the effect of the air quality ensuring measures during the game period using the tropospheric NO_2 column density retrieved from Ozone Monitoring Instrument (OMI) onboard AURA satellite. About 40% reduction in tropospheric NO_2 column density over the Beijing area is obtained from the assessment during July to August, 2008, a key period of air quality ensuring measures for the Beijing 2008 Olympic Games.

4. Conclusion

China hosted XXIX Olympic and Paralympics Games in its capital, Beijing, from August to September of 2008. To improve the air quality during this period, extreme stringent pollutions control policies were applied to Beijing and its neighbouring provinces. A variety of optical remote sensing techniques were employed on the measurements of the air quality of Beijing at different stages of Olympic Games. The aerosol extinction coefficients and aerosol optical depth between August 7th and August 25th were obtained using Raman LIDAR. Differential Optical Absorption Spectroscopy (DOAS) was utilized to evaluate the density of SO_2, NO_2, O_3. The density of SO_2, NO_2, O_3 from July 20th to August 24th were reduced by 14%-33%, 15%-61%, and 2.5%-14%, than that of July 1st to July 19th, respectively. The troposphere NO_2 column density acquired using multi-axis differential DOAS (MAX-DOAS) was found to be much higher than that from OMI with a maximum factor of 2.4. PM_{10} was found to decline by 10% - 12% during the Olympic Game period using TEOM. The results were compared with data from other groups using similar methods or different methods like satellite observations or air quality modelling system, and demonstrated the efficiency of pollution control measures to improve the air quality during the XXIX Olympic Games in 2008.

Using the optical remote techniques aforementioned along with other techniques like satellite observation, an integrated spatiotemporal monitoring system for regional complex air pollution was constructed. The results demonstrated the efficiency of pollution control measures in surrounding areas in improving air quality in Beijing. Optical remote sensing techniques were proved to be critical in air quality monitoring system.

5. Acknowledgment

6. References

Cermak, J., & Knutti, R. (2009). Beijing olympics as an aerosol field experiment. *Geophysical Research Letters*, 36, L10806.

Chen, Z. Y., Liu, W. Q., Zhang, Y. J., Zhao, N. J., He, J. F., & Ruan, J. (2009). Measurements of aerosol distribution by an elastic-backscatter lidar in summer 2008 in beijing. *Chinese Optics Letters*, 7, 753-755.

Duncan, B. N., Yoshida, Y., Olson, J. R., Sillman, S., Martin, R. V., Lamsal, L., et al. (2010). Application of omi observations to a space-based indicator of nox and voc controls on surface ozone formation. *Atmospheric Environment*, 44, 2213-2223.

He, S. Z., Chen, Z. M., Zhang, X., Zhao, Y., Huang, D. M., Zhao, J. N., et al. (2010). Measurement of atmospheric hydrogen peroxide and organic peroxides in beijing before and during the 2008 olympic games: Chemical and physical factors influencing their concentrations. *Journal of Geophysical Research-Atmospheres*, 115.

He, Y., Zhang, Y. J., Kan, R. F., Xia, H., Geng, H., Ruan, J., et al. (2009). Open-path online monitoring of ambient atmospheric co2 based on laser absorption spectrum. *Spectroscopy and Spectral Analysis*, 29, 10-13.

He, Y. B., Kan, R. F., Englich, F. V., Liu, W. Q., & Orr, B. J. (2010). Simultaneous multi-laser, multi-species trace-level sensing of gas mixtures by rapidly swept continuous-wave cavity-ringdown spectroscopy. *Optics Express*, 18, 20059-20071.

Hou, Q., An, X. Q., Wang, Y., & Guo, J. P. (2010). An evaluation of resident exposure to respirable particulate matter and health economic loss in beijing during beijing 2008 olympic games. *Science of the Total Environment*, 408, 4026-4032.

Huang, X. F., He, L. Y., Hu, M., Canagaratna, M. R., Sun, Y., Zhang, Q., et al. (2010). Highly time-resolved chemical characterization of atmospheric submicron particles during 2008 beijing olympic games using an aerodyne high-resolution aerosol mass spectrometer. *Atmospheric Chemistry and Physics*, 10, 8933-8945.

Jin, L., Gao, M. G., Liu, W. Q., Lu, Y. H., Zhang, Y. J., Wang, Y. P., et al. (2010). Application of sof-ftir method to measuring ammonia emission flux of chemical plant. *Spectroscopy and Spectral Analysis*, 30, 1478-1481.

Lackner, M. (2007). Tunable diode laser absorption spectroscopy (tdlas) in the process industries - a review. *Reviews in Chemical Engineering*, 23, 65-147.

Li, S. W., Liu, W. Q., Xie, P. H., Wang, F. S., & Yang, Y. J. (2009). Real-time forecasting model for monitoring pollutant with differential optical absorption spectroscopy. *Spectroscopy and Spectral Analysis*, 29, 3057-3060.

Li, S. W., Liu, W. Q., Xie, P. N., Li, A., Qin, M., Peng, F. M., et al. (2008). Observation of the nighttime nitrate radical in hefei, china. *Journal of Environmental Sciences-China*, 20, 45-49.

Li, Y., Shao, M., Lu, S. H., Chang, C. C., & Dasgupta, P. K. (2010). Variations and sources of ambient formaldehyde for the 2008 beijing olympic games. *Atmospheric Environment*, 44, 2632-2639.

Liu, J. F., Mu, Y. J., Zhang, Y. J., Zhang, Z. M., Wang, X. K., Liu, Y. J., et al. (2009). Atmospheric levels of btex compounds during the 2008 olympic games in the urban area of beijing. *Science of the Total Environment*, 408, 109-116.

Liu, X. G., Zhang, Y. H., Jung, J. S., Gu, J. W., Li, Y. P., Guo, S., et al. (2009). Research on the hygroscopic properties of aerosols by measurement and modeling during carebeijing-2006. *Journal of Geophysical Research-Atmospheres*, 114.

Lu, C. P., Liu, W. Q., Zhao, N. J., Liu, L. T., Chen, D., Zhang, Y. J., et al. (2010a). Influence of humidity on characteristic of laser-induced soil plasmas. *Spectroscopy and Spectral Analysis*, 30, 2885-2888.

Lu, C. P., Liu, W. Q., Zhao, N. J., Liu, L. T., Chen, D., Zhang, Y. J., et al. (2010b). Measurement and analysis of copper in soil using laser-induced breakdown spectroscopy. *Spectroscopy and Spectral Analysis*, 30, 3132-3135.

Luo, Y. H., Liu, W. Q., Bian, L. G., Lu, C. G., Xie, P. H., Si, F. Q., et al. (2011). The retrieval of ozone column densities by passive differential optical absorption spectroscopy during summer at zhongshan station, antarctic. *Spectroscopy and Spectral Analysis*, 31, 456-460.

Mijling, B., van der A, R. J., Boersma, K. F., Van Roozendael, M., De Smedt, I., & Kelder, H. M. (2009). Reductions of no2 detected from space during the 2008 beijing olympic games. *Geophysical Research Letters*, 36.

Movasaghi, Z., Rehman, S., & Rehman, I. U. (2008). Fourier transform infrared (ftir) spectroscopy of biological tissues. *Applied Spectroscopy Reviews*, 43, 134-179.

Patashnick, H., & Rupprecht, E. G. (1991). Continuous pm-10 measurements using the tapered element oscillating microbalance. *Journal of the Air & Waste Management Association*, 41, 1079-1083.

Shao, M., Lu, S. H., Liu, Y., Xie, X., Chang, C. C., Huang, S., et al. (2009). Volatile organic compounds measured in summer in beijing and their role in ground-level ozone formation. *Journal of Geophysical Research-Atmospheres*, 114.

Shen, J. L., Tang, A. H., Liu, X. J., Kopsch, J., Fangmeier, A., Goulding, K., et al. (2011). Impacts of pollution controls on air quality in beijing during the 2008 olympic games. *Journal of Environmental Quality*, 40, 37-45.

Shou-bin, F., Gang, T., Gang, L., Yu-hu, H., Jian-ping, Q., & Shui-yuan, C. (2009). Road fugitive dust emission characteristics in beijing during olympics game 2008 in beijing, china. *Atmospheric Environment*, 43, 6003-6010.

Si, F. Q., Xie, P. H., Dou, K., Zhan, K., Liu, Y., Xu, J., et al. (2010). Determination of the atmospheric aerosol optical density by multi axis differential optical absorption spectroscopy. *Acta Physica Sinica*, 59, 2867-2872.

Simonich, S. L. M. (2009). Response to comments on "atmospheric particulate matter pollution during the 2008 beijing olympics". *Environmental Science & Technology*, 43, 7590-7591.

Streets, D. G., Fu, J. S., Jang, C. J., Hao, J. M., He, K. B., Tang, X. Y., et al. (2007). Air quality during the 2008 beijing olympic games. *Atmospheric Environment*, 41, 480-492.

Tang, X. Y., Shao, M., Hu, M., Wang, Z. F., & Zhang, J. F. (2009). Comment on "atmospheric particulate matter pollution during the 2008 beijing olympics". *Environmental Science & Technology*, 43, 7588-7588.

Tang, Y. Y., Liu, W. Q., Kan, R. F., Zhang, Y. J., Liu, J. G., Xu, Z. Y., et al. (2010). Spectroscopy processing for the NO measurement based on the room-temperature pulsed quantum cascade laser. *Acta Physica Sinica*, 59, 2364-2368.

Vierling, K. T., Vierling, L. A., Gould, W. A., Martinuzzi, S., & Clawges, R. M. (2008). Lidar: Shedding new light on habitat characterization and modeling. *Frontiers in Ecology and the Environment*, 6, 90-98.

Wang, B., Shao, M., Lu, S. H., Yuan, B., Zhao, Y., Wang, M., et al. (2010). Variation of ambient non-methane hydrocarbons in beijing city in summer 2008. *Atmospheric Chemistry and Physics*, 10, 5911-5923.

Wang, M., Zhu, T., Zheng, J., Zhang, R. Y., Zhang, S. Q., Xie, X. X., et al. (2009). Use of a mobile laboratory to evaluate changes in on-road air pollutants during the beijing 2008 summer olympics. *Atmospheric Chemistry and Physics*, 9, 8247-8263.

Wang, S. X., Zhao, M., Xing, J., Wu, Y., Zhou, Y., Lei, Y., et al. (2010). Quantifying the air pollutants emission reduction during the 2008 olympic games in beijing. *Environmental Science & Technology*, 44, 2490-2496.

Wang, T., Nie, W., Gao, J., Xue, L. K., Gao, X. M., Wang, X. F., et al. (2010). Air quality during the 2008 beijing olympics: Secondary pollutants and regional impact. *Atmospheric Chemistry and Physics*, 10, 7603-7615.

Wang, T., & Xie, S. D. (2009). Assessment of traffic-related air pollution in the urban streets before and during the 2008 beijing olympic games traffic control period. *Atmospheric Environment*, 43, 5682-5690.

Wang, W. T., Primbs, T., Tao, S., & Simonich, S. L. M. (2009). Atmospheric particulate matter pollution during the 2008 beijing olympics. *Environmental Science & Technology*, 43, 5314-5320.

Wang, X., Westerdahl, D., Chen, L. C., Wu, Y., Hao, J. M., Pan, X. C., et al. (2009). Evaluating the air quality impacts of the 2008 beijing olympic games: On-road emission factors and black carbon profiles. *Atmospheric Environment*, 43, 4535-4543.

Westerdahl, D., Wang, X., Pan, X. C., & Zhang, K. M. (2009). Characterization of on-road vehicle emission factors and microenvironmental air quality in beijing, china. *Atmospheric Environment*, 43, 697-705.

Winer, A. M., & Biermann, H. W. (1994). Long pathlength differential optical-absorption spectroscopy (doas) measurements of gaseous hono, no2 and hcho in the california south coast air basin. *Research on Chemical Intermediates*, 20, 423-445.

Xin, J. Y., Wang, Y. S., Tang, G. Q., Wang, L. L., Sun, Y., Wang, Y. H., et al. (2010). Variability and reduction of atmospheric pollutants in beijing and its surrounding area during the beijing 2008 olympic games. *Chinese Science Bulletin*, 55, 1937-1944.

Xu, J., Xie, P. H., Si, F. Q., Dou, K., Li, A., Liu, Y., et al. (2010). Retrieval of tropospheric no2 by multi axis differential optical absorption spectroscopy. *Spectroscopy and Spectral Analysis*, 30, 2464-2469.

Xu, Z. Y., Liu, W. Q., Kan, R. F., Zhang, Y. J., Liu, J. G., Zhang, S. A., et al. (2010). Study on the arithmetic of absorbance inversion based on tunable diode-laser absorption spectroscopy. *Spectroscopy and Spectral Analysis*, 30, 2201-2204.

Yang, T., Wang, Z. F., Zhang, B., Wang, X. Q., Wang, W., Gbauidi, A., et al. (2010). Evaluation of the effect of air pollution control during the beijing 2008 olympic games using lidar data. *Chinese Science Bulletin*, 55, 1311-1316.

Yao, X. H., Xu, X. H., Sabaliauskas, K., & Fang, M. (2009). Comment on "atmospheric particulate matter pollution during the 2008 beijing olympics". *Environmental Science & Technology*, 43, 7589-7589.

Yu, H., Wang, P. C., Zong, X. M., Li, X., & Lu, D. R. (2010). Change of no2 column density over beijing from satellite measurement during the beijing 2008 olympic games. *Chinese Science Bulletin*, 55, 308-313.

Zhang, L. F., Huang, Y. R., Shi, S. X., Zhou, L., Zhang, T., Dong, L. A., et al. (2010). Concentration and gas-particle partitioning of hexachlorobenzene in the ambient air before and after the beijing olympic games. *Bulletin of Environmental Contamination and Toxicology*, 85, 1-4.

Zhang, S. A., Dong, F. Z., Zhang, Z. R., Wang, Y., Kan, R. F., Zhang, Y. J., et al. (2009). Monitoring of oxygen concentration based on tunable diode laser absorption spectroscopy. *Spectroscopy and Spectral Analysis*, 29, 2593-2596.

Zhou, Y., Wu, Y., Yang, L., Fu, L. X., He, K. B., Wang, S. X., et al. (2010). The impact of transportation control measures on emission reductions during the 2008 olympic games in beijing, china. *Atmospheric Environment*, 44, 285-293.

Zhu, Y. W., Liu, W. Q., Xie, P. H., Dou, K., Qin, M., & Si, F. Q. (2010). Monitoring and analysis for vertical profiles of air pollutants in boundary layer of beijing. *Chinese Journal of Geophysics-Chinese Edition*, 53, 1278-1283.
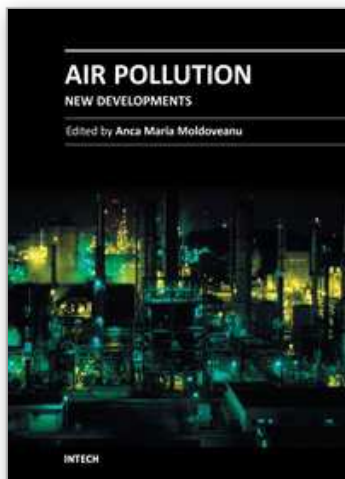
Air Pollution - New Developments

Edited by Prof. Anca Moldoveanu

Today, an important issue is environmental pollution, especially air pollution. Due to pollutants present in air, human health as well as animal health and vegetation may suffer. The book can be divided in two parts. The first half presents how the environmental modifications induced by air pollution can have an impact on human health by inducing modifications in different organs and systems and leading to human pathology. This part also presents how environmental modifications induced by air pollution can influence human health during pregnancy. The second half of the book presents the influence of environmental pollution on animal health and vegetation and how this impact can be assessed (the use of the micronucleus tests on TRADESCANTIA to evaluate the genotoxic effects of air pollution, the use of transplanted lichen PSEUDEVERNIA FURFURACEA for biomonitoring the presence of heavy metals, the monitoring of epiphytic lichen biodiversity to detect environmental quality and air pollution, etc). The book is recommended to professionals interested in health and environmental issues.

How to reference

In order to correctly reference this scholarly work, feel free to copy and paste the following:

INTECH

open science | open minds